Improved Clamped Z-Source Converter with Optimized Maximum Power Point Tracker for Hybrid Renewable Energy Systems Based Energy Management System

Saranya M.[1], Giftson S. G.[2]
[1]Arasu Engineering College, Kumbakonam, Tamilnadu, India.
[2]Sir Issac Newton College of Engineering and Technology, Nagapattinam, Tamilnadu, India.

Abstract. In light of the intermittent and seasonal nature of wind and solar energy, electrical systems are becoming more problematic to operate. The purpose of the work is to establish an energy storage system that helps to minimize such operational challenges, which are essential to improve grid stability and reliability. The tasks solved in the article to achieve the given goal are the following: incorporating an energy management system with the aid of improved converter and optimized maximum power point (MPPT) for (Photovoltaic) PV and PMSG (permanent magnet synchronous generator) based wind system. On comparing with conventional Z-source converters, a novel improved clamped Z-source converter, which is utilized in this work has high efficiency with low THD and it has the capacity to protect electrical circuits against damage caused by short circuits, overcurrent and overvoltage. The Pulse Width Modulation (PWM) rectifier is implemented to convert AC-DC supply obtained from the PMSG wind system. Firefly optimization with an aid of Radial Basis Function Neural Network (RBFNN) technique is employed as an MPPT system for extracting optimal power from photovoltaic system. The excess energy obtained from the hybrid sources are stored in the battery and it is controlled by the recurrent neural network (RNN) with the bidirectional converter. The overall developed system is executed in MATLAB software and the most important outcomes are demonstrated in terms of high efficiency with 91.2%, high tracking efficiency of 98.54% and reduced THD of 2.45% respectively. The significance of results obtained in this research lies in the advancement of renewable energy integration technologies. By overcoming the challenges associated with intermittent energy sources, the developed system contributes to the improvement of grid stability and reliability.
Keywords**:** synchronous generator maximum power point, improved clamped Z-source converter, firefly optimized neural network, recurrent neural network.

DOI: https://doi.org/10.52254/1857-0070.2024.1-61.05
UDC: **621.314.572**

Convertorul îmbunătățit de limitare a impedanței cu sistemul optimizat de urmărire a punctului de putere maximă pentru sistemul de control al unui sistem combinat de alimentare cu surse de energie regenerabile

Saranya M.[1], Giftson S. G.[2]
[1]Arasu Engineering College, Kumbakonam, Tamilnadu, India
[2]Colegiul Sir Issac Newton de Inginerie și Tehnologie, Nagapattinam, Tamilnadu, India

Rezumat. Datorită naturii intermitente și sezoniere a energiei eoliene și solare, operarea sistemelor electrice devine din ce în ce mai dificilă. Integrarea sistemelor de stocare a energiei poate minimiza aceste probleme operaționale pentru a îmbunătăți stabilitatea și fiabilitatea rețelei. În acest sens, lucrarea propusă implementează un sistem de management al energiei folosind un convertor avansat și un sistem optimizat de control al punctului de putere maximă pentru sisteme fotovoltaice și eoliene bazat pe un generator sincron cu magnet permanent. Un convertor de impedanță de limitare a sursei Z nou și îmbunătățit este utilizat pentru a crește puterea de ieșire a sistemului fotovoltaic și pentru a asigura o eficiență ridicată, iar un redresor cu modulație de lățime a impulsurilor (RMI) este utilizat pentru a converti puterea AC în DC de la sistemul de energie eoliană. Optimizarea prin metoda ”flacără-fluturaș” cuplată cu funcția de bază radială rețeaua neuronală este utilizată ca sistem de urmărire pentru a optimiza punctul de putere maximă pentru a obține puterea optimă din sistemul fotovoltaic. Excesul de energie obținut din surse hibride de energie regenerabilă este stocat într-o baterie și controlat de o rețea neuronală recurentă folosind un convertor bidirecțional. Semnificația rezultatelor obținute este îmbunătățirea calității tensiunii de ieșire a sistemului de alimentare, reducerea coeficientului de distorsiune neliniară și creșterea eficienței conversiei.
Cuvinte cheie: punct de putere maximă generator sincron, convertor de sursă Z-îmbunătățită, rețea neuronală optimizată fluturaș, rețea neuronală recurentă.

Модифицированный ограничивающий импедансный преобразователь с оптимизированной следящей системой за точкой максимальной мощности для системы управления комбинированной системой энергоснабжения с ВИЭ

Сарания М.[1], Гифтсон С. Д.[2]

[1]Инженерный колледж Арасу, Кумбаконам, Тамилнаду, Индия

[2]Инженерно-технологический колледж им. сэра Иссака Ньютона, Нагапаттинам, Тамилнаду, Индия

Аннотация. Ввиду прерывистого и сезонного характера ветровой и солнечной энергии эксплуатация электрических систем становится все более проблематичной. Интеграция систем хранения энергии позволяет свести к минимуму подобные эксплуатационные проблемы, что необходимо для повышения стабильности и надежности электросети. В связи с этим в предлагаемой работе реализована система управления энергопотреблением с помощью усовершенствованного преобразователя и оптимизированной системы управления точкой максимальной мощности для фотоэлектрической и ветровой систем на базе синхронного генератора с постоянными магнитами). Для увеличения выходной мощности фотоэлектрической системы и обеспечения ее высокого КПД используется новый улучшенный импедансный преобразователь с ограничивающим Z-источником, а для преобразования переменного тока в постоянный, получаемого от энергосистемы с ветрогенератором, применяется выпрямитель с широтно-импульсной модуляцией (ШИМ). В качестве следящей системы для оптимизации точки максимальной мощности для получения оптимальной мощности от фотоэлектрической системы используется оптимизация с помощью метода "пламя-светлячок" совместно с использованием нейронной сети с радиальной базисной функцией. Избыточная энергия, полученная от гибридных источников возобновляемой энергии, накапливается в аккумуляторе и управляется рекуррентной нейронной сетью с помощью двунаправленного преобразователя. Значимость полученных результатов состоит в повышении качества выходного напряжения энергосистемы, снижения коэффициента нелинейных искажений и повышения КПД преобразования.

Ключевые слова: точка максимальной мощности синхронного генератора, улучшенный преобразователь Z-источника, нейронная сеть, рекуррентная нейронная сеть.

I. INTRODUCTION

The world's energy demand has raised as a consequence of rapid urbanization and population growth [1]. There is a tendency to choose an alternate source of power generation owing to the ongoing exhaustion of fossil fuels and its detrimental effects on atmosphere [2]. The Development of Renewable Energy Sources (RES) is gaining a lot of attention for the purpose of overcoming the drawbacks of fossil fuels. The five types of RES are biomass, solar, wind, tidal, and wave. From that Solar and wind energy are used to generate electricity since they are abundant and easily accessible [3-4].Dependability of solar and wind energy is significantly impacted by climate variability and unpredictable nature. As a result, it raises fundamental issues related to grid integration [5]. Hybridizing RESs with energy storage is a possible solution to conquer aforestated issues and it stores excess primary energy when it is practicable and supports the renewable energy shortage when necessary. Flexible energy management solutions from the battery system boost the power quality of hybrid systems for producing electricity from renewable sources [6-7].

A DC/DC converter is necessary for hybrid power systems with low output terminal voltage of Photovoltaic system [8]. There are various DC-DC converters used for applications involving RES such as [9] boost, buck [10], buck-boost, Cuk [11] and SEPIC [12].The Boost and Buck approaches among these converters have low-order circuits, excellent efficiency, and simplicity. The battery cannot be charged continuously with MPPT operation using both Boost and Buck converters [13]. Since the Buck-Boost, SEPIC, Zeta, and Cuk converters produce an output voltage that generate an enhanced voltage with high efficiency, which attain MPP tracking irrespective of variations in the climate as well as the linked load. Nevertheless, those converters exhibited ripples current and gets fluctuating performance in MPPT [14-15].Consequently, the improved clamped Z-source converter is employed in this proposed work, which generates reduced ripples harmonics with high efficiency.

In spite of fluctuating operating points and changing climatic conditions, several MPPT algorithms are utilized to keep the extracted power from the array at its maximum level [16]. The most frequently used techniques are conventional ones, including INC (Incremental Conductance) and P&O (Perturb and Observe). The MPP could only be tracked by conventional methods provided the weather remained steady,

despite its straightforward construction and application [17]. Additionally, conventional MPPT algorithms have oscillations close to MPP and are ineffective for large-scale solar power systems. The world's researchers are developing new strategies for managing MPPT in solar systems as a result of aforementioned constraints. Heuristic approaches like genetic algorithms (GA), Particle Swarm Optimization (PSO), Fuzzy Logic Controls (FLC), Artificial Neural Networks (ANN) are the most common advanced MPPT techniques. Unfortunately, these MPPT algorithms are more expensive to implement, which need a precise training dataset and are more complex [19-20]. The limitations occurred by the aforesaid topologies are overcome by the proposed topology with the aid of Firefly optimized RBFNN based MPPT techniques, which effectively tracked the ideal power from PV system. The objectives of implemented work illustrates below,

- To improve energy management system by using PV and PMSG based wind system.
- To augment optimal power from PV with high efficiency by adopting Improved clamped Z-source converter.
- To extract optimal power from PV by utilizing Firefly optimized RBFNN based MPPT technique.
- To store excess energy from PV by employing battery together with RNN Controller for effectual control.

II. PROPOSED METHODOLOGY

The HRES are employed for generating power due to their availability in abundance. The dependability of solar and wind energy is simultaneously impacted by climatic changes and irregularity. Henceforth, the proposed work establishes improved clamped Z-source converter with optimized MPPT topologies for effective grid performance, which contributes to the enhancement of grid stability and reliability. The implemented work's block diagram is specified in Fig. 1 and is explained below.

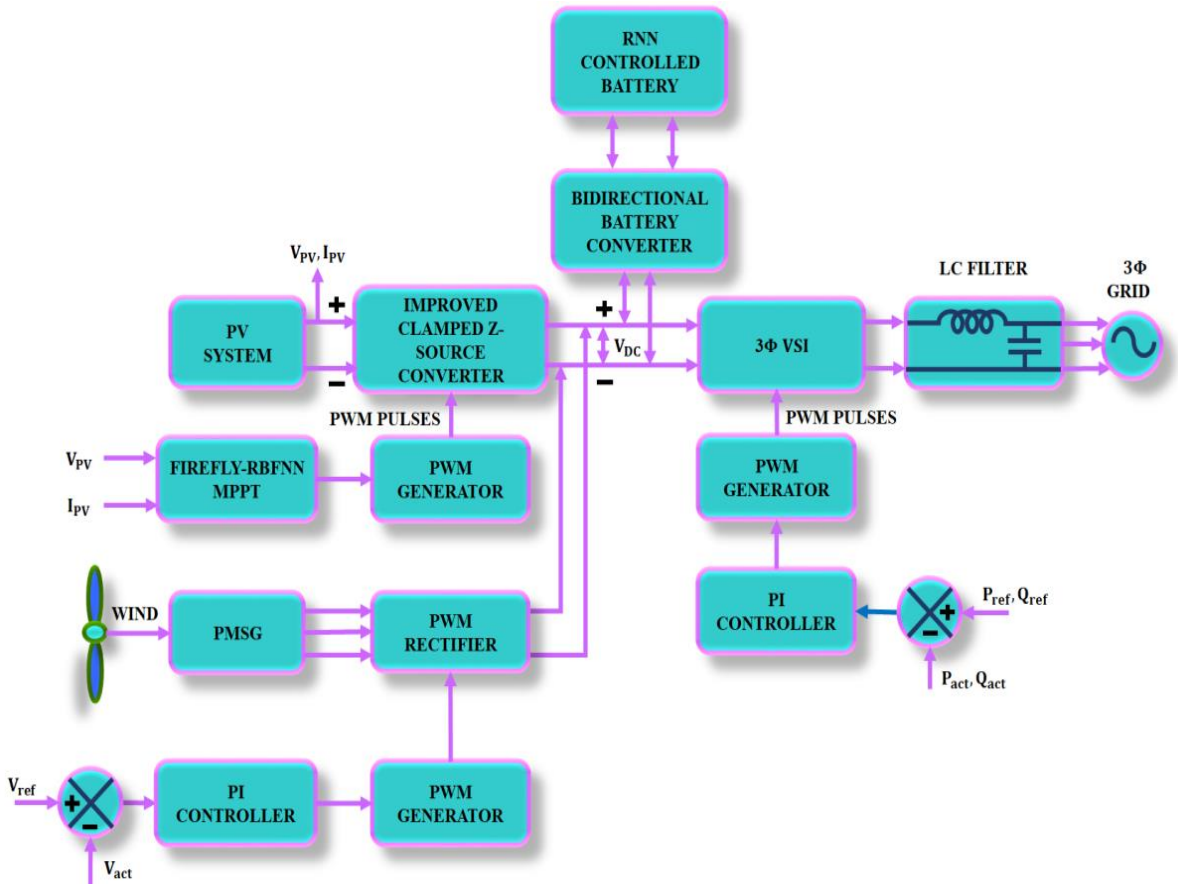

Fig. 1. Block diagram for the proposed topology.

At first, the low output voltage of Photovoltaic system is supplied to the improved clamped Z-source converter for boosting low voltage from PV system. The output voltage V_{PV} and current I_{PV} is given as input to the Firefly optimized RBFNN based MPPT topology for

tracking maximum power from the Photovoltaic system. The optimal power is fed to PWM generator, which generates PWM pulses for better functioning of developed converter. In addition to PV system, the proposed work implements PMSG-wind system. The AC supply from wind system is converted into DC supply using PWM rectifier. After that, the actual and reference voltage is compared, which generate error signal and it is fed to the PI controller for error compensation. Then the controlled output is fed to the PWM generator for better working of rectifier and the stabilized voltage is deliver to the DC-link.

Moreover, the extra energy from PV system is preserved in Bidirectional battery converter and it is controlled by RNN controller, the stored energy in battery can be utilized in the time of lagging energy. Furthermore, the DC-link voltage is given to 3ΦVSI for converting DC-AC supply, after that the actual and reference is compared, which produce the error signal and it is compensated by adopting the PI controller. The controlled output is fed to PWM generator for producing PWM pulses. Finally, uninterruptable and constant power is distributed to three-phase grid with the aid of LC filter.

A. Modelling Of PV System

In Fig. 2, the PV source displays a single diode model. It provides specific output traits of several PV cell and module types.

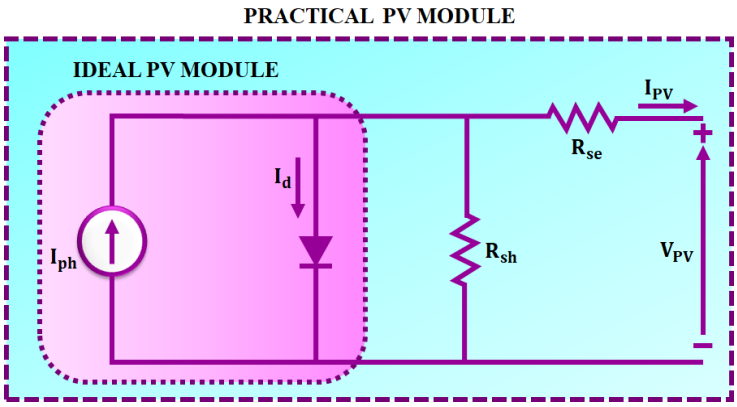

Fig. 2. Circuit diagram of PV Module.

This model has diode, shunt resistance R_{sh}, series resistance R_{se} and current source I_{ph}, following values are provided for the gross module output current I_{PV}:

$$I_{PV} = I_{ph} - I_d - \frac{V_{PV} + R_{se} I_{PV}}{R_{sh}} \tag{1}$$

Where, the diode current I_d and the current caused by the incidence of light at level G, I_{ph} are represented as,

$$\begin{cases} I_{ph} = \left[I_{ph,n} + K_1 \left(T - T_n \right) \right] \dfrac{G}{G_n} \\ I_d = I_{rs} \left[exp\left(\dfrac{V_{PV} + R_{se} I_{PV}}{\xi V_t} \right) - 1 \right] \end{cases} \tag{2}$$

The following are the values for thermal voltage V_t at temperature T as well as the diode reverse saturation current I_{rs} for N_{se} series-connected cells:

$$\begin{cases} V_t = N_{se} KT / q \\ I_{rs} = \dfrac{I_{sc,n} + K_1 \left(T - T_n \right)}{exp\left(\dfrac{V_{oc,n} + K_V \left(T - T_n \right)}{\xi V_t} \right) - 1} \end{cases} \tag{3}$$

Where V_{PV} denoted as a PV module's output voltage; $I_{ph,n}$ indicates current produced by light under the usual test conditions. T_n, G_n, $I_{sc,n}$ and $V_{oc,n}$ denotes a temperature, irradiance, short circuit current as well as open circuit voltage at *STC* correspondingly. Boltzmann constant is represents the *k*, *q*, electron charge as well as the diode ideality constant. K_1 and K_V specify the short circuit current as well as open circuit voltage temperature coefficients.

Following this, to extract optimum power from Photovoltaic system, the RBFNN based MPPT technique is implemented, which is explained below.

B. Modelling Of RBFNN Based MPPT Technique

The method used in this developed work is called Radial Basis Function Neural Networks, and it is a model of a simple neural network design with input, hidden, and output layers. A RBFNN-based MPPT method is intended to make possible to control MPPT without being aware of the ecological changes in PV system. Because this study's purpose is to extract optimal power from the Photovoltaic system. The structure of RBFNN based MPPT is represented in Fig. 3. The data will be used to implement the RBFNN, which will replace the outdated MPPT block. Three levels comprise the RBFNN. With only the input signal being matched, the first layer is an input player. There may be a number of factors, each of which is associated with a different neuron. Each hidden layer neuron's input receives values from the input layer neurons' outputs.

$$\left.\begin{aligned} net_j^{\,1} &= x_i^{\,1} \\ y_{1j}^{\,1} &= f^{\,1}\left(net_j^{\,1}\right) = \left(x_i^{\,1}\right) \end{aligned}\right\}_{j=1..n,i=1,2} \tag{4}$$

Here, $f\left(x_i^{\,1}\right)$ specifies the sum of nodes $x_i^{\,1}$ denotes the input layer, which is given to the hidden layer. The centers and spreads of network are chosen during the training phase. The net input and output of the hidden layer are displayed below,

$$\left.\begin{aligned} net_j^{\,2} &= \sum_j W_{1j}^{\,1} y_{1j}^{\,1} \\ y_{1j}^{\,2} &= f^{\,2}\left(W_{1j}^{\,1} y_{1j}^{\,1} + b_j^{\,1}\right) \end{aligned}\right\}_{j=1...n} \tag{5}$$

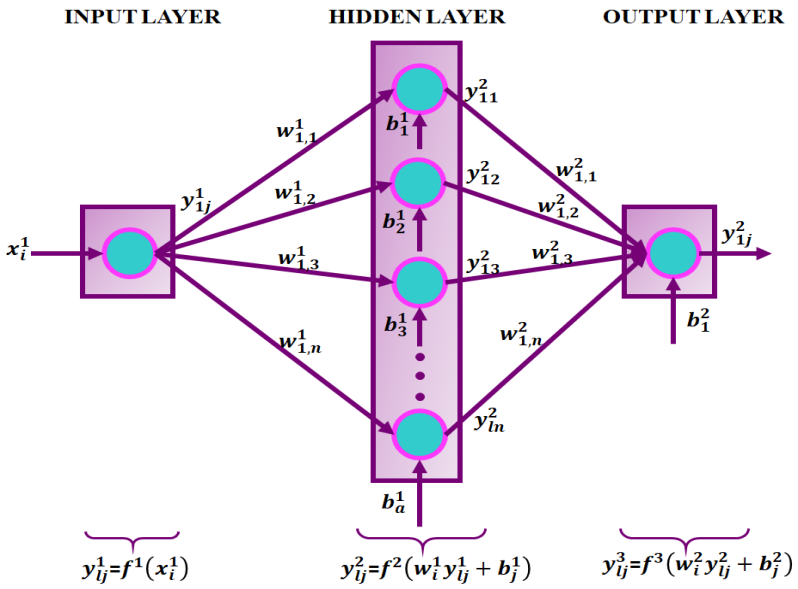

Fig. 3. Schematic diagram of RBFNN based MPPT.

Where, the bias term of hidden is specified as $b_j^{\,1}$ and $W_{1j}^{\,1}$ indicates the weight that connect the input and hidden layer.

Only the hidden as well as output layer weights are changed and calculated during training as below,

$$\left.\begin{aligned} net_j^{\,3} &= \sum_j W_{1j}^{\,2} y_{1j}^{\,2} \\ y_{1j}^{\,3} &= f^{\,3}\left(W_{1j}^{\,2} y_{1j}^{\,2} + b_j^{\,2}\right) \end{aligned}\right\}_{j=1...n} \tag{6}$$

The RBFNN based MPPT topology gets trained accurately at the same time tuning is essential.

Hence, the proposed work implemented the Firefly optimization topology.

Firefly Optimization

The FFA optimization technique was developed to replicate how fireflies use flashing lights to attract one another. The metaheuristic is primarily effective at resolving numerical optimization issues and takes inspiration from the flashing behaviour of fireflies. This population-based method works under the presumption that the quality of the agent representing the problem solution determines how bright it "glows “In the processes of competition and cooperation, the firefly individuals will gravitate toward the

brighter one in search of the population's ideal solution. The individual quality and evolution direction of fireflies are determined by their brightness value, while the distance and speed between individual fireflies and the population's ideal solution are determined by their appeal value. The performance of the FA throughout the search phase depends on the light intensity and attraction value. The flowchart of the proposed Firefly optimized RBFNN based MPPT is represented in Fig. 4.

The following expressions represent each firefly's relative brightness and seduction.

$$I = I_0 e^{-\gamma r_{i,j}} \tag{7}$$

$$\beta = \beta_0 e^{-\gamma r^2_{i,j}} \tag{8}$$

Here, γ specifies the light absorption coefficient, r_{ij} indicates the Cartesian distance between two fireflies, β_0 denotes the maximum attraction and I_0 represents the maximum initial brightness of fireflies.

$$x_{i+1} = x_i + \beta\left(x_j - x_i\right) + \alpha\left(rand - \frac{1}{2}\right) \tag{9}$$

Where, x_i and x_j specifies the spatial position of fireflies, rand indicates the random number within [0, 1] and α denotes the step factor. In reality, each of the fireflies stand in for a particular RBF network in a classification. The best firefly vectors i for a given trained RBF network maximize the fitness function as specified in Equation 9 below.

$$f\left(t_i\right) = \frac{1}{1 + MSE} \tag{10}$$

To enhance the low output power of PV, the improved clamped Z-source converter is implemented and it is described below.

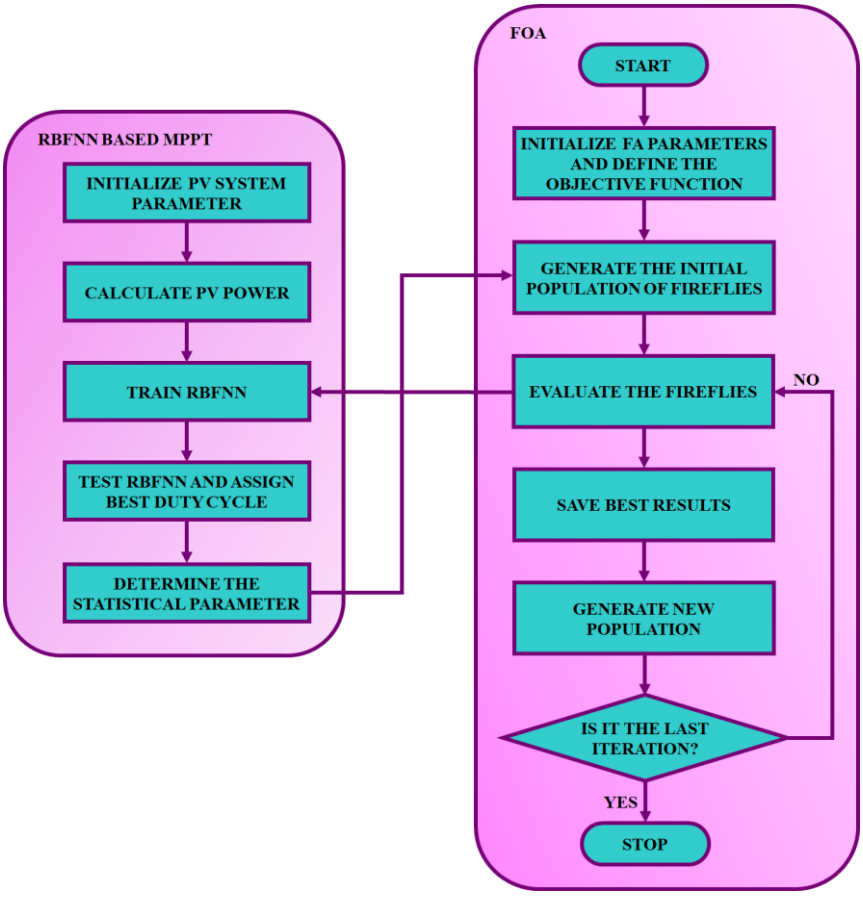

Fig. 4. Flowchart of Firefly Optimized RBFNN based MPPT.

C. Modelling Of Improved Clamped Z-Source Converter

a) Clamped Z-source converter

The clamped Z-source converter uses a larger modulation index with fewer components to provide high voltage gain, which reduces the shoot-through duty cycle. Less shoot through duty

cycle is used by this converter with equivalent input or output states, which reduces voltage stress and improves power quality output. It contains 2 diode, 3 inductor, 2 capacitor and 1 switch. In this research work, a novel improved clamped Z-source converter is employed, which has the capacity to protect electrical circuits against damage caused by short circuits, overcurrent and overvoltage.

b) Improved Clamped Z-source converter

Fig. 5 represents the circuit design of the implemented improved clamped Z-source converter. The inductors are charged in parallel and discharged in series to obtain a high voltage gain. This converter contains two inductors, four diodes, two capacitors and one switch. Compare to clamped Z-source converter, the proposed converter has 4 diodes, hence it has the capacity to protect electrical circuits against damage caused by short circuits, overvoltage as well as overcurrent.

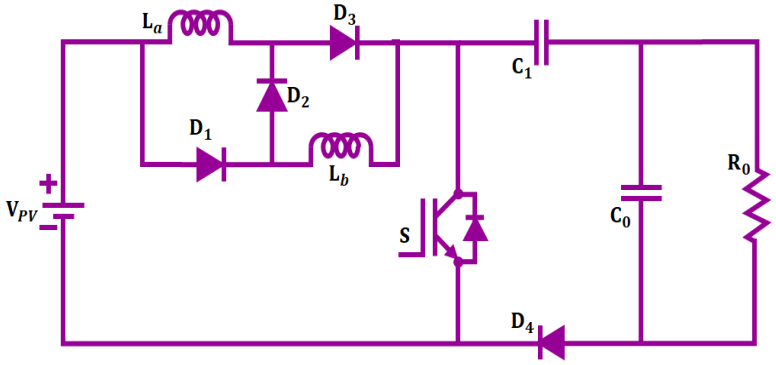

Fig. 5. Circuit diagram of Improved Clamped Z-source converter.

Mode 1: Switch is ON condition- when Switch is ON condition diode D_2 *and* D_4 gets OFF state as specified in Fig.6 (a). At this mode, the inductors L_a *and* L_b charge over the diode D_3*and* D_1. The diodes D_2*and* D_4 and is in forward biased because of its low potential current and the flow of current is illustrated in figure, from which C_1 gets charge through D_3 and the output capacitor C_0 stores the energy. The diode D_1 and capacitor C_1 are connected in series with the source during the first mode to supply the necessary energy to the load via the switch.

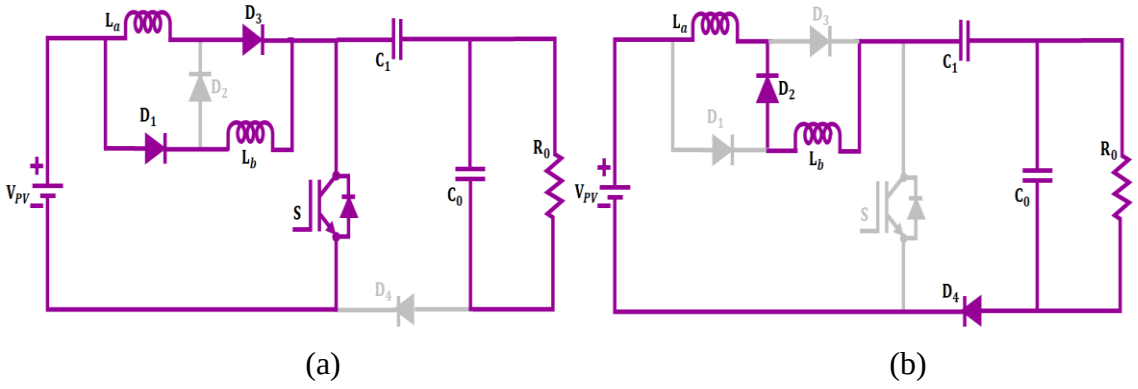

Fig. 6. Modes of Operation (a) ON and (b) OFF condition.

Mode 2: Switch is in OFF condition: During switch in OFF condition, the diode D_3*and* D_1 gets OFF condition as represents in Fig. 6 (b).

At this stage, both the inductors starts to discharge thorough the diode D_2*and* D_4 as well as the clamp capacitor C_1.

The capacitor C_1 receives a channel through the diode D_4 from the inductors' discharging current. The output capacitor distributes the energy needed by the load during OFF condition.

There are two distinct operating modes for converters. Fig. 7 illustrates the anticipated waveform.

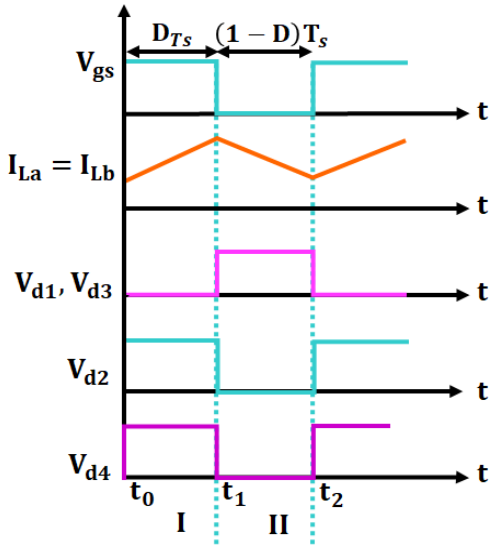

Fig. 7. Waveform for the proposed converter.

Mathematical model of proposed converter

By using Kirchhoff's voltage law, the inductor voltages V_{La} and V_{Lb} is expressed in below equation at Mode 1,

$$V_{La} = V_{Lb} = V_{in} \tag{11}$$

The developed improved clamped Z-source converter output voltage is determined by adopting the subsequent equation at Mode 1,

$$V_{out} = V_{in} + V_{c1} \tag{12}$$

By using Kirchhoff's voltage law, at Mode 2expressed in below equation,

$$V_{La} + V_{Lb} = V_{in} - V_{c1} \tag{13}$$

The voltage over the capacitor V_{c1} is stated as,

$$V_{c1} + V_{in} + V_{d3} + V_{d1} \tag{14}$$

The diode voltage stresses, V_{d1} and V_{d3} are expressed as below,

$$V_{d1} = V_{d3} = \frac{D}{1-D} V_{in} \tag{15}$$

The developed converter output voltage equation, V_{out} is attained by substituting Equations (13) and (14) in Equation (11). It is provided as follows,

$$V_{out} = V_{in} + V_{in} + \frac{D}{1-D} + \frac{D}{1-D} V_{in} = \frac{2}{1-D} V_{in} \tag{16}$$

Thus, theoretical voltage gain, M of implemented converter expresses as below,

$$M = \frac{V_{out}}{V_{in}} = \frac{2}{1-D} \tag{17}$$

The voltage over the switch S, V_{ds} and diode V_{d4} is written as,

$$V_{ds} = V_{d4} = V_{in} + V_{d3} + V_{d1} = \frac{1+D}{1-D} V_{in} \tag{18}$$

By adopting the proposed improved clamped Z-source converter the high efficiency with reduced switching losses is attained.

D. Modelling Of PMSG Based Wind System

WT model

The mechanical output power of the wind turbine is supplied by,

$$P_m = \frac{1}{2} \rho \pi R^2 C_p(\alpha, \beta) v_w^{\,2} \tag{19}$$

Here, ρ denotes the air density, C_p specifies the power coefficient function, α indicates tip speed ratio, v_w denotes wind speed and β specifies blade pitch angle. Power coefficient and tip speed ratio are written as below,

$$\alpha = \frac{\omega_t}{v_w} R \tag{20}$$

Here, the angular speed of rotor indicates ω_t.

PMSG Model

Fig.3 shows the PMSG's analogous circuit model. Stator voltage of the PMSG wind turbine is provided by,

$$\begin{cases} u_{ds} = R_s i_{ds} + L_{ds} \dfrac{di_{ds}}{dt} - \omega_r L_{qs} i_{qs} \\ u_{qs} = R_s i_{qs} + L_{qs} \dfrac{di_{qs}}{dt} - L_{ds} i_{ds} \omega_r + \lambda_r \omega_r \end{cases} \tag{21}$$

Here, L_{ds} and L_{qs} specifies synchronous inductances of generator on d, q axis, u_{ds} and u_{qs} indicates stator terminal voltages, ω_r denotes the electrical angular velocity, λ_r represents amplitude of flux linkage. The active as well as reactive powers at generator terminals as well as the electromagnetic torque of the generator, are presented as.

$$T_e = \frac{3}{2} \rho i_{qs} \lambda_r \tag{22}$$

$$\begin{bmatrix} P \\ Q \end{bmatrix} = \frac{3}{2} u_{ds} \begin{bmatrix} i_{ds} \\ i_{qs} \end{bmatrix} + \frac{3}{2} u_{qs} \begin{bmatrix} i_{qs} \\ -i_{ds} \end{bmatrix} \quad (23)$$

Here, P denotes the number of poles, T_e indicates the torque. Fig. 8 presents the equivalent circuit model of PMSG.

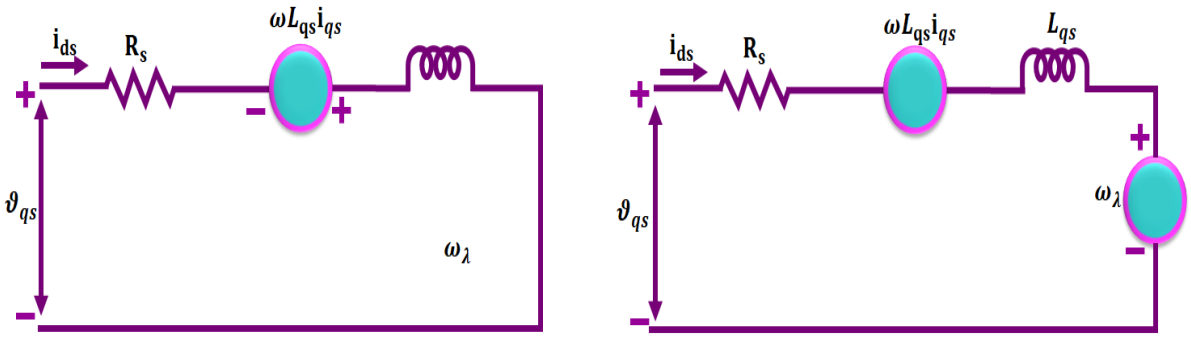

(a) **(b)**

Fig. 8. Equivalent circuit model (a) d-axis (b) q-axis circuit.

The AC supply generated by the PMSG wind system is converted in to DC with the aid of PWM rectifier and the PI controller is utilized for regulating the rectifier, which is described as follows.

E. Modelling of PI controller

To guarantee the DC link voltage dynamic stability in the event of step load variation or line voltage fluctuation, PI controllers have been employed. The outermost DC voltage controller's PI form can be expressed as follows:

$$C\frac{dV_{dc}}{dt} = K_{pv}\left(V_{dc}^{*} - V_{dc}\right) + \frac{K_{Iv}}{s}\left(V_{dc}^{*} - V_{dc}\right) \quad (24)$$

Here, K_{Iv} and K_{pv} specifies the integral and proportional coefficient, V_{dc} indicates the output DC voltage, V_{dc}^{*} specifies reference output DC voltage.

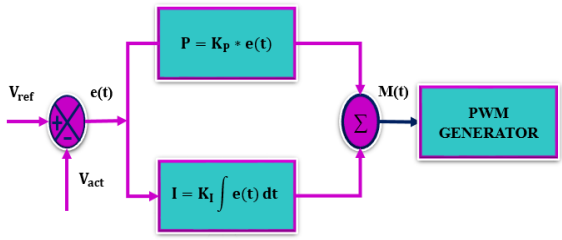

Fig. 9. Structure of PI controller.

To store additional energy from the Hybrid PV and PMSG based wind system, the battery is developed, to control the battery RNN controller is implemented that is explained below,

F. Modelling of RNN Controlled Battery

In relation to the accessibility of renewable models, the load demand swings as well as the load diagram. According to this supposition, the RNN modelling approach can be used to formulate the problem of the BESS control strategy. The power provided by BESS during discharge is fed in charge mode as well as presently recognised by foremost RNN is,

$$P_{BESS} = V_{Bn} I_{BESS} \quad (25)$$

After that, the electric current designed as,

$$I_{BESS} = \frac{P_{BESS}}{V_{Bn}} \quad (26)$$

The second RNN receives this value as an input, and it uses that value to calculate the voltage at the moment. In order to manage BESS, this latter is employed in conjunction with the SOC.

G. Modelling of Bidirectional Converter

Fig. 9 depicts the non-isolated bidirectional DC-DC converter. Let's first examine the two ways of Buck and Boost Mode, in which this converter operates. For the bidirectional operation in this case, controlled switches are used in place of diodes. Switch S1 turns on for Buck mode, while Switch S2 goes OFF for Boost mode. **Buck mode:** In the Buck mode, an output voltage is less than the input voltage. The battery will be charged off via the DC grid. The input current increases when switch S1 is ON and passes via S1 and L. Up until the following cycle, the inductor current decreases while S1 is OFF. Inductor L provides the energy needed to charge the battery.

Boost mode: When in boost mode, an output voltage is greater than input voltage. The battery's power is fed to the load. The input current increases through the switches S2 and S2 while switch S2 is ON. The inductor current lowers till the next cycle when S2 is turned off. The load is subject to the flow of energy from inductor L.

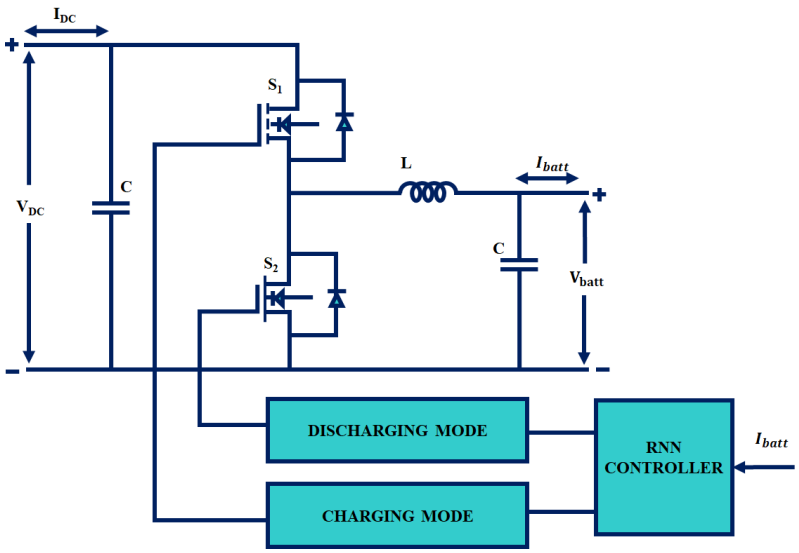

Fig. 10. Diagram of Bidirectional Battery converter.

III. RESULTS AND DISCUSSION

In this work, an energy management system incorporates with the aid of improved clamped Z-source converter and Firefly optimized RBFNN based MPPT for PV and PMSG based wind system. By adopting the battery controlled system, the excess energy from the hybrid sources are effectively stored. The developed model executed in MATLAB/Simulink to show the developed system's proficiency and comparative analysis is carried out for the significance of implemented topology. Table 1 describes the parameter specification for the implemented work.

Table 1
Parameter specification

Parameters	**specification**
PV system	
No. of Panels	20 *panels*
Open circuit voltage	22.6V
Peak power	10 kW
Series connected solar PV cells	36
Short circuit voltage	12V
PMSG	
Power	10 kW
No. of Turbines	1
Voltage	575V
Improved Clamped Z-source converter	
C_1	4.7μF
C_0	2200 μF
L_a, L_b	1.2mH
Switching frequency f	10kHz

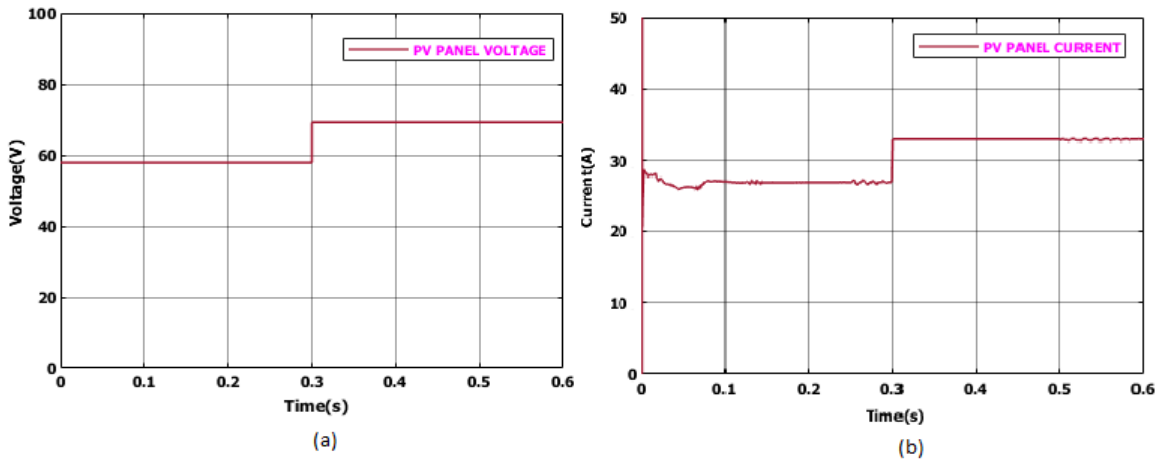

Fig.11.PV panel Waveform for (a) Voltage and (b) Current.

Fig. 11 illustrates the PV panel waveform for the developed work, which is observed that initially the voltage fluctuates and continuously upheld at 75V after 0.3s as indicated in Fig.11 (a). As well the current is varied initially and after 0.3s it constantly maintained 33A and minor oscillation occurs after 0.5s as represents in Fig. 11 (b).

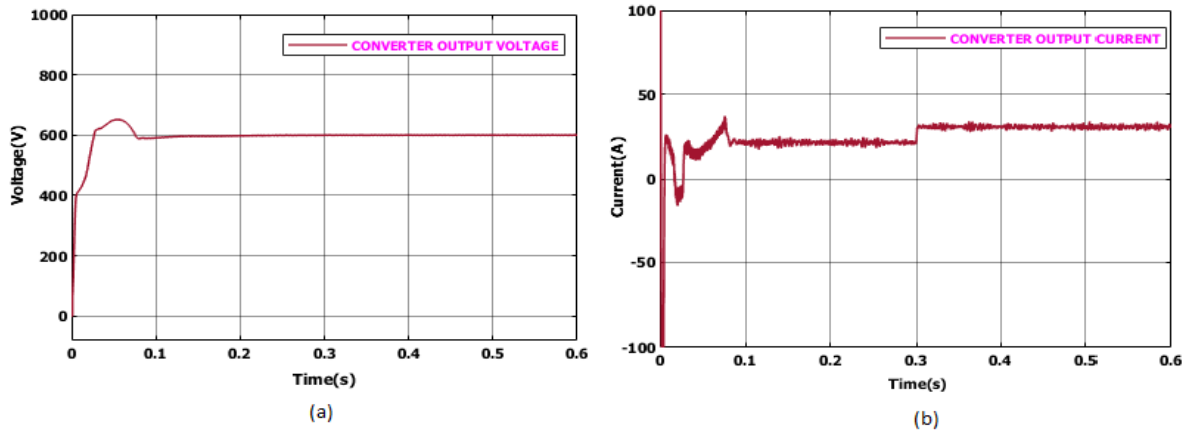

Fig. 12. Converter output waveform for (a) Voltage and (b) Current.

Fig. 12 represents converter output waveform for the implemented work, it is analysed that initially the voltage fluctuates and suddenly raised at 600V after 0.2s and constantly maintained as represented in Fig.12 (a). By observing Fig. 12 (b), the current fluctuates initially after 0.3s peakly raised and constantly maintained at 45A with minor distortion.

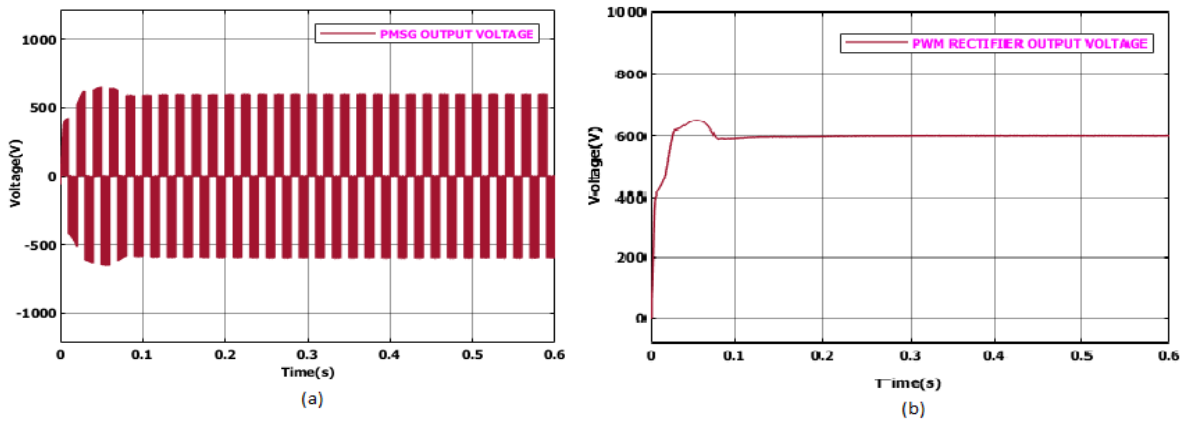

Fig. 13. Output waveform for (a) PMSG voltage and (b) PWM rectifier voltage.

The output waveform for PMSG and PWM rectifier is represents in Fig. 13, which is analysed that the output voltage of PMSG is slightly fluctuates initially and gradually maintained at 600V to -600V after 0.1s as represents in Fig. 13(a). As well Fig. 13 (b) noted that the voltage of PWM rectifier fluctuated initially and suddenly raised after 0.1s then constantly maintained at 600V.

Waveform for battery is represented in Fig. 14, which is observed that the SOC is constantly upheld at 60% as indicates in Fig. 14 (a). From Fig. 14 (b), the voltage of battery is continually upheld at 125V as well the current of battery fluctuates initially and suddenly dropped at 3A after 0.2s as denoted in Fig. 14 (c).

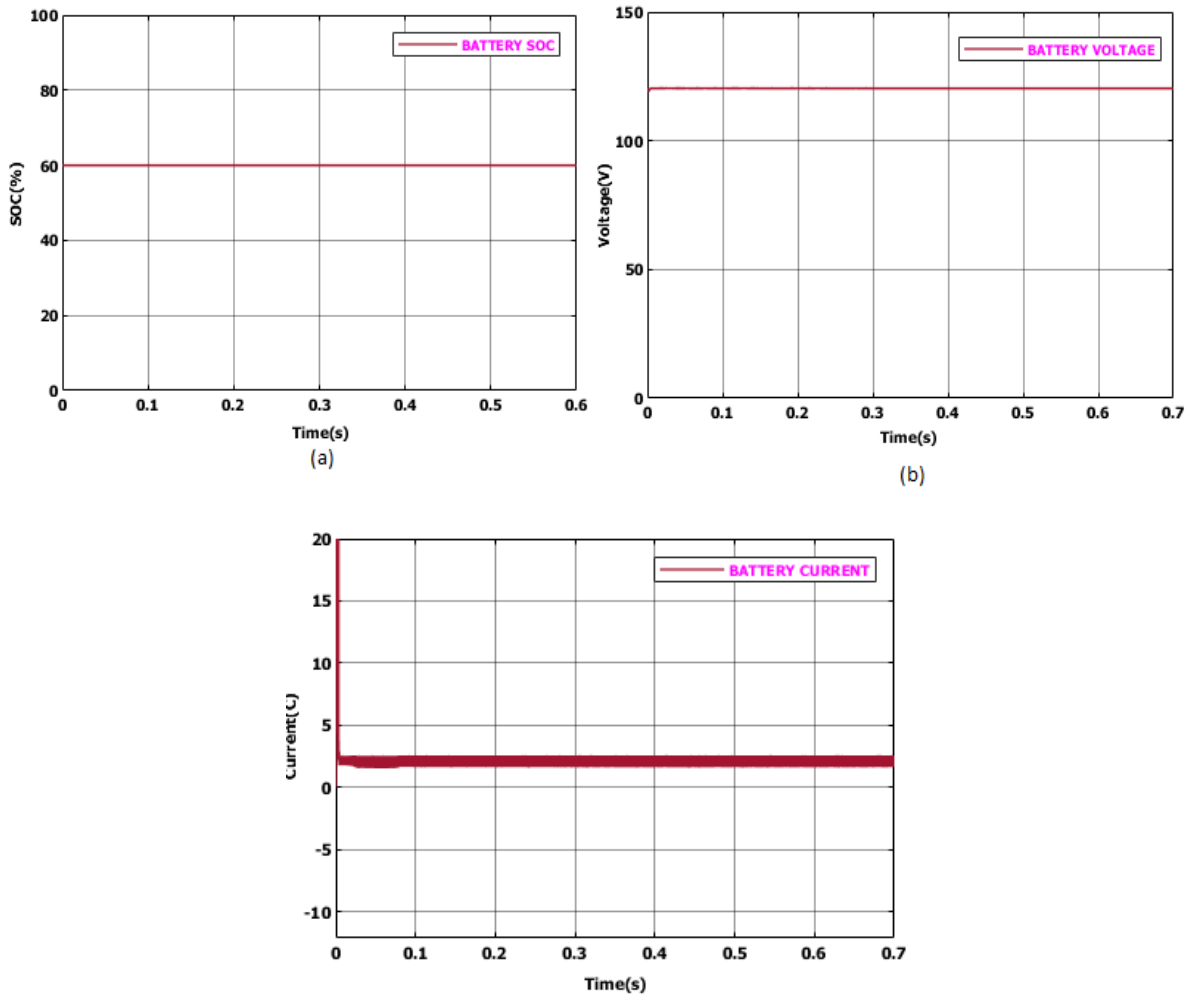

Fig. 14. Waveform for Battery (a) SOC (b) Voltage and (c) Current.

The waveform of grid is represented in Fig. 15, from the waveform it is analysed that voltage is gradually continued at 400V to -400V as illustrates in Fig. 15 (a). Likewise, in Fig. 15 (b) the current constantly upheld at 13A to -13A.The grid voltage and current inphase waveform, which represents the ideal power factor, is displayed in Fig. 15(c).

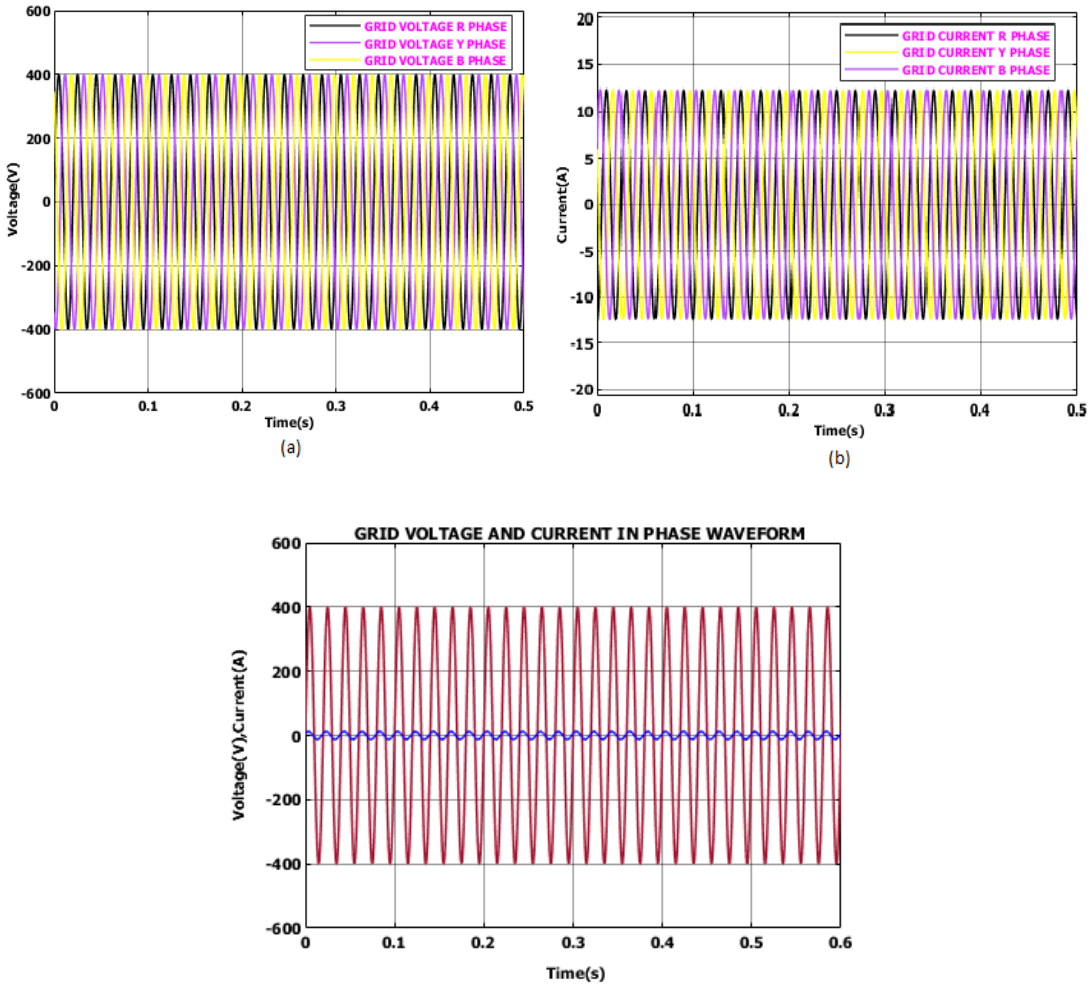

Fig. 15. Waveform for grid (a) Voltage (b) Current and (c) grid voltage and current inphase.

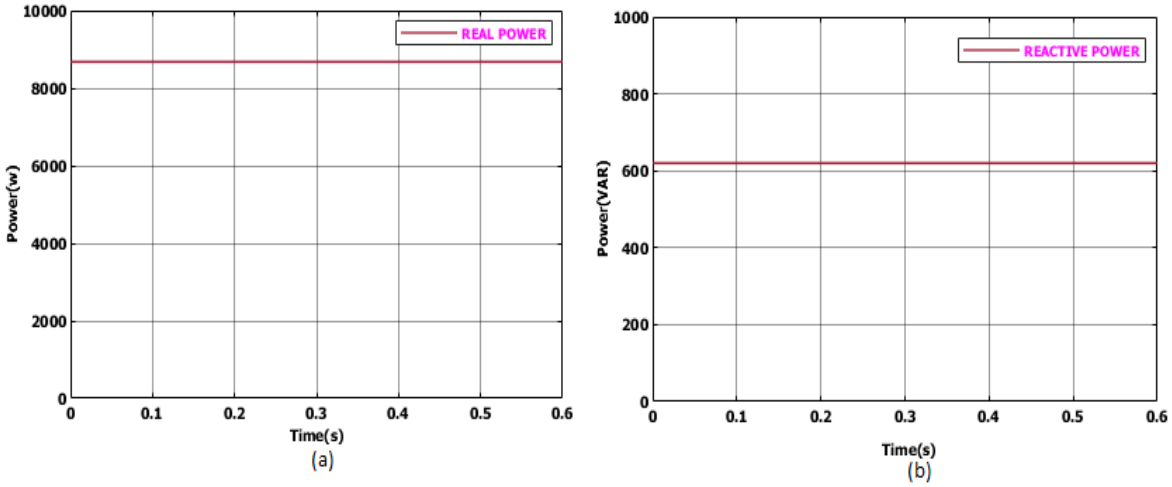

Fig. 16.Waveform for (a) Real power and (b) Reactive power.

The reactive and real power waveform for the developed work is illustrated in Fig. 16.From the waveform, the real power and reactive power waveform is accomplished at unity as depicted in Fig. 16 (b) the power constantly maintained at 610(VAR).

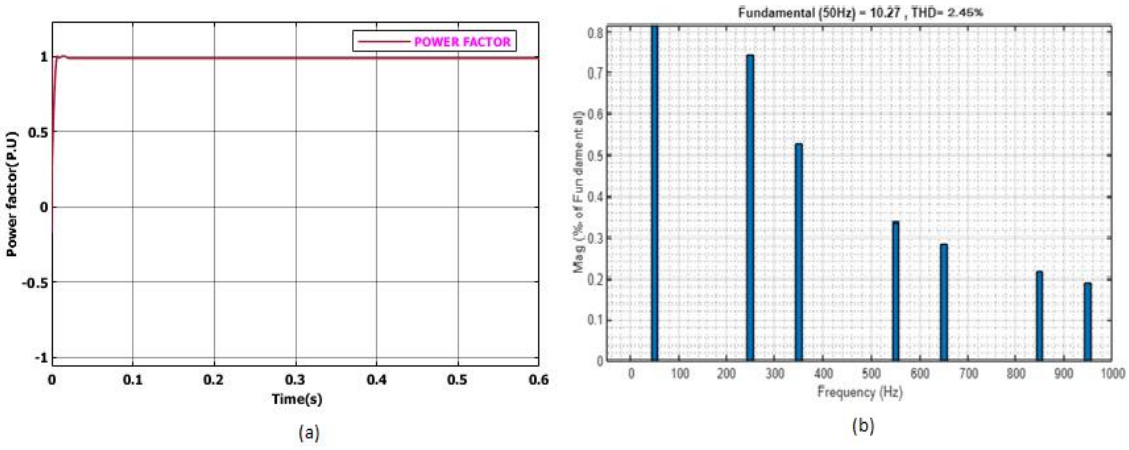

Fig. 17. Waveform form (a) Power factor and (b) THD.

Fig. 17 represented Power factor and THD waveform, which is analysed that a power factor value of unity is accomplished. As represented in Fig. 17 (b), the THD waveform for the developed work attains 2.45%.

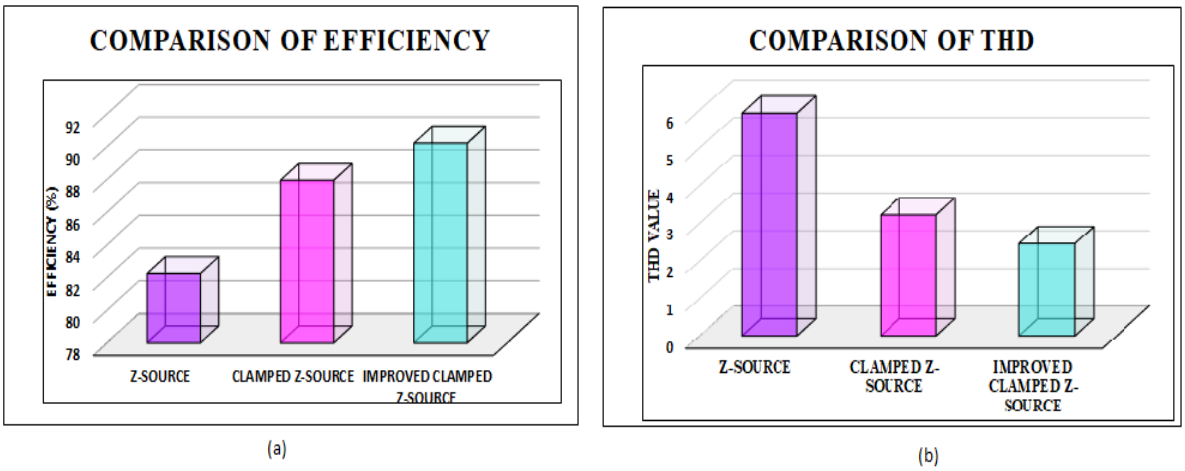

Fig. 18. Comparison for (a) Efficiency and (b) THD value.

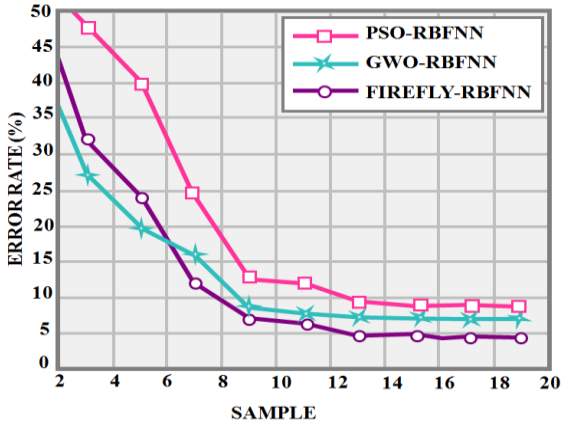

Fig.19. Comparison of Error rate.

The efficiency and THD value is compared with the conventional converters like Z-source as well as Clamped Z-source, from the Fig. 18 (a) it is observed that proposed Improved Clamped Z-source converter attains high efficiency of 91.2% and the low THD value of 2.45% is attained as specifies in Fig. 18 (b).

Table 2
Comparison of tracking efficiency with various MPPT topologies

MPPT Techniques	Tracking Efficiency (%)
P&O [21]	95%
ABO [22]	97%
PSO [23]	98.25 %
MFO [24]	98.31%
Proposed Firefly – RBFNN based MPPT	98.54%

The comparison of error rate is depicted in Fig. 19, from which it is analysed that compared to the other optimized techniques like PSO-RBFNN, GWO-RBFNN, the proposed Firefly optimized RBFNN achieved lower error than the conventional approaches.

The tracking efficiency of proposed optimized MPPT is compared with the existing approaches like P&O, ABO, PSO and MFO. Comparing the developed optimized RBFNN based MPPT system to the existing topologies, it can be observed from the table analysis that the system achieves a high tracking efficiency of 98.54%.

IV. CONCLUSION

In this analyzation, the proposed work incorporate HRES for energy management system with the aid of improved Clamped Z-source converter and Firefly optimized RBFNN based MPPT. By implementing Optimized RBFNN based MPPT technique, the optimal power from the PV system is efficiently extracted. Moreover, the low output voltage from PV system is proficiently boosted by adopting improved Clamped Z-source converter with high efficiency. The excess energy from the hybrid RES are stored in battery and it is powerfully controlled by the RNN with the Bidirectional Battery converter. The developed work is performed out by utilizing MATLAB/Simulink to reveal the developed system's performance. As a consequence, Comparative analysis is made to foreshow the proficiency of implemented work. Which concluded that by utilizing the proposed work high efficiency of 91.2%, Low THD of 2.45%, high tracking efficiency of 96.54%, rapid convergence speed is achieved when compare to the other converter and optimized topologies. Finally, the developed work distributes the uninterruptable power supply to grid system with improved grid stability and reliability.

References

[1] Al-Ammar E. A., Habib H. U. R., Kotb K. M., Wang S., Ko W., Elmorshedy M. F., Waqar A. Residential community load management based on optimal design of standalone HRES with model predictive control. *IEEE Access*, 2020, vol. 8, pp. 12542-12572.

[2] Salama H. S., Said S. M., Aly M., Vokony I., Hartmann B. Studying impacts of electric vehicle functionalities in wind energy-powered utility grids with energy storage device. *IEEE Access*, 2021, vol. 9, pp. 45754-45769.

[3] Kavin K. S., SubhaKaruvelam P. PV-based grid interactive PMBLDC electric vehicle with high gain interleaved DC-DC SEPIC Converter. *IETE Journal of Research*, 2023, vol. 69, no. 7, pp. 4791-4805.

[4] Haegel N. M., Kurtz S. R. Global Progress toward Renewable Electricity: Tracking the Role of Solar (Version 3). *IEEE Journal of Photovoltaics*, 2023.

[5] Kumar P. S., Chandrasena R. P. S., Ramu V., Srinivas G. N., Babu K. V. S. M. Energy management system for small scale hybrid wind solar battery based microgrid. *IEEE Access*, 2020, vol. 8, pp. 8336-8345.

[6] Tsai C. T., Beza T. M., Molla E. M., Kuo C. C. Analysis and sizing of mini-grid hybrid renewable energy system for islands. *IEEE Access*, 2020, vol. 8, pp. 70013-70029.

[7] Banu J. B., Muthuramalingam M., Nammalvar P. ANFIS based double integral sliding mode control for a grid-integrated hybrid power system. *Optik*, 2022, vol. 270, pp. 170013.

[8] HuX., Liu X., Zhang Y., Yu Z., Jiang S. A hybrid cascaded high step-up DC–DC converter with ultralow voltage stress. *IEEE Journal of Emerging and Selected Topics in Power Electronics*, 2020, vol. 9, no. 2, pp. 1824-1836.

[9] Ahmad J., Pervez I., Sarwar A., Tariq M., Fahad M., Chakrabortty R. K., Ryan M. J. Performance analysis and hardware-in-the-loop (HIL) validation of single switch high voltage gain DC-DC converters for MPP tracking in solar PV system. *IEEE Access*, 2020, vol. 9, pp. 48811-48830.

[10] Hussein B., Alsalemi A., Ben-Brahim L. High-Gain Non-isolated Single-Switch DC-DC Converters in Power Factor Correction Rectifiers: A Performance Assessment. In *2022 3rd International Conference on Smart Grid and Renewable Energy (SGRE)*, 2022, pp. 1-6. IEEE, 2022.

[11] Chandrasekar B., Nallaperumal C., Padmanaban S., Bhaskar M. S., Holm-Nielsen J. B., Leonowicz Z., Masebinu S. O. Non-isolated high-gain triple port DC–DC buck-boost converter with positive output voltage for photovoltaic applications. *IEEE Access*, 2020, vol. 8, pp. 113649-113666.

[12] Andrade A. M. S. S., Faistel T. M. K., Toebe A., Guisso R. A. Family of transformerless active switched inductor and switched capacitor Ćuk DC–DC converter for high voltage gain applications. *IEEE Journal of Emerging and Selected Topics in Industrial Electronics*, 2021, vol. 2, no. 4, pp. 390-398.

[13] Hasanpour S., Forouzesh M., Siwakoti Y. P., Blaabjerg F. A new high-gain, high-efficiency SEPIC-based DC–DC converter for renewable energy applications. *IEEE Journal of Emerging and Selected Topics in Industrial Electronics*, 2021, vol. 2, no. 4, pp. 567-578.

[14] Saranya M., Samuel G. G. Energy management in hybrid photovoltaic–wind system using optimized neural network. *Electrical Engineering*, 2023, pp. 1-18.

[15] Seguel J. L., Seleme Jr, S. I., Morais L. M. Comparative study of Buck-Boost, SEPIC, Cuk and Zeta DC-DC converters using different MPPT methods for photovoltaic applications. *Energies*, 2022, vol. 15, no. 21, pp. 7936.

[16] Chandrasekar B., Nallaperumal C., Padmanaban S., Bhaskar M. S., Holm-Nielsen J. B., Leonowicz Z., Masebinu S. O. Non-isolated high-gain triple port DC–DC buck-boost converter with positive output voltage for photovoltaic applications. *IEEE Access*, 2020, vol. 8, pp. 113649-113666.

[17] Osmani K., Haddad A., Lemenand T., Castanier B., Ramadan M. An investigation on maximum power extraction algorithms from PV systems with corresponding DC-DC converters. *Energy*, 2021, vol. 224, pp. 120092.

[18] Ali A., Almutairi K., Padmanaban S., Tirth V., Algarni S., Irshad K., Islam S., Zahir M. H., Shafiullah M., Malik M.Z. Investigation of MPPT techniques under uniform and non-uniform solar irradiation condition–a retrospection. *IEEE Access*, 2020, vol. 8, pp. 127368-127392.

[19] Zhang Y., Wang Y. J., Zhang Y., Yu T. Photovoltaic fuzzy logical control MPPT based on adaptive genetic simulated annealing algorithm-optimized BP neural network. *Processes*, 2022, vol. 10, no. 7, pp. 1411.

[20] Katche M. L., Makokha A. B., Zachary S. O., Adaramola M. S. A comprehensive review of maximum power point tracking (mppt) techniques used in solar PV systems. *Energies*, 2023, vol. 16, no. 5, pp. 2206.

[21] Millah I. S., Chang P. C., Teshome D. F., Subroto R. K., Lian K. L., Lin J. F. An enhanced grey wolf optimization algorithm for photovoltaic maximum power point tracking control under partial shading conditions. *IEEE Open Journal of the Industrial Electronics Society*, 2022, vol. 3, pp. 392-408.

[22] Manoharan P., Subramaniam U., Babu T. S., Padmanaban S., Holm-Nielsen J. B., Mitolo M., Ravichandran S. Improved perturb and observation maximum power point tracking technique for solar photovoltaic power generation systems. *IEEE Systems Journal*, 2020, vol. 15, no. 2, pp. 3024-3035.

[23] Senthilkumar S., Mohan V., Mangaiyarkarasi S. P., Karthikeyan M. Analysis of single-diode PV model and optimized MPPT model for different environmental conditions. *International Transactions on Electrical Energy Systems*, 2022.

[24] Rezk H., Zaky M. M., Alhaider M., Tolba M. A. Robust Fractional MPPT-Based Moth-Flame Optimization Algorithm for Thermoelectric Generation Applications. *Energies*, 2022, vol. 15, no. 23, pp. 8836.

Information about authors.

Mani Saranya received her UG degree in B.E. (Electrical and Electronics Engineering) in 2006 at Dhanalakshmi Srinivasan Engineering College, perambalur. She also received her PG degree in (Power Systems Engineering) in 2011 at College of Engineering Guindy, Chennai. She is working as a assistant Professor, in Department of Electrical and Electronics Engineering, Arasu Engineering College, Kumbakonam. She has 16 years experience in the teaching field.
E-mail: saranyam111.eee@gmail.com

Dr. George Giftson Samuel received his B.E (Electrical and Electronics Engineering) degree from Madurai Kamaraj University, Madurai, Tamilnadu, India. He received his M.E (Power Electronics) degree and Ph.D (Power system) degree from Anna University Chennai. He is working as a Professor in the Department of Electrical and Electronics Engineering, Sir Issac Newton College of Engineering and Technology, Nagapattinam. He has published many technical papers in various International and National Journals and Conferences. His research interest includes Energy Management and Optimization. He is a senior member of IEEE USA, a member of IAENG, Hong Kong, a member of the Indian society of Technical Education, and a fellow of the Institution of Engineers, India. E-mail: giftsam2k@gmail.com